Available online at www.sciencedirect.com
ScienceDirect
International Journal of Thermal Sciences 48 (2009) 165–173
International Journal of Thermal Sciences
www.elsevier.com/locate/ijts

Effect of excess air on grate combustion of solid wastes and on gaseous products

Thomas Rogaume [a,*], F. Jabouille [a], J.L. Torero [b]

[a] *Laboratoire de Combustion et de Détonique, ENSMA, BP 40109, 86961 Futuroscope Cedex, France*
[b] *School of Engineering and Electronics, The University of Edinburgh, Edinburgh, EH9 3JN, UK*

Received 13 June 2007; received in revised form 7 February 2008; accepted 7 February 2008

Available online 14 March 2008

Abstract

An experimental study has been conducted in a fixed bed reactor to simulate, in a laboratory scale, industrial municipal waste incineration using moving grates. Carbon monoxide, nitrogen oxide, temperatures and mass loss rate measurements have been used to establish the importance of the operating parameters of a municipal waste incinerator in the characteristics of the combustion process. The present work is concerning the study of the impact of primary and secondary airs of combustion. Two different regimes have been identified that are controlled by the airflow through the fuel (primary airflow). These combustion regimes have indicated the impact of primary and secondary air flow on the combustion behavior and the resulting concentrations of carbon monoxide and nitrogen oxide: the production of NO seems to be controlled only by the oxygen concentration in the secondary zone of combustion. An increase in total airflow, thus, results in an increase in the yield of NO.
© 2008 Elsevier Masson SAS. All rights reserved.

Keywords: Combustion; Municipal solid wastes; NOx; Carbon monoxide; Primary air; Secondary air; Excess air; Regime of combustion

1. Introduction

Urban waste management is an increasingly difficult process. Incineration is one of the most commonly employed techniques in Europe, mainly because it can permit a reduction of 70% of the mass and 90% of the volume of the waste, but also because the calorific output of European waste is consistent with power generation schemes. However, the biggest challenge remains on the generation of pollution during the incineration of the waste, either through gaseous emissions or ashes. In-depth reviews are provided by [1,2]. Among the major environmental concerns related to incineration are the emissions of nitrogen oxides.

During the incineration of municipal solid waste in grid furnace incinerators, NO is the major component of the NO_x formed, representing 95% of those emissions [3]. Therefore, it is justifiable to concentrate only on the establishment of the main variables controlling NO. Past studies have shown that NO is generated from three sources: thermal NO [4], prompt NO [5] and fuel NO [6,7]. Temperatures required for significant formation of prompt and thermal NO tend to be higher than 1500 K [7], this is not the case in a municipal solid waste furnace [8–10]. Furthermore, the combustion of waste is generally lean as shown by typical residual oxygen levels comprised between 6 and 12%. It is therefore expected that the quantity of NO formed by means of those mechanisms to be negligible [9–11]. The main formation path for nitrogen monoxide during incineration of municipal solid waste is through the fuel-NO mechanism.

Recent works has shown that during the combustion of the volatile matters emanating from municipal solid waste more than 95% of the NO formed originated from the fuel [11,12]. The formation of NO from the fuel has been well described [6,7,9]. The study of the formation mechanisms shows that radicals like $O^{\cdot}$ or $OH^{\cdot}$ strongly participate in the formation of NO. Therefore, the local content of oxygen has an important influence on the production of NO via the fuel mechanism as well as the composition of the gases coming from the thermal degradation of the solid fuels.

* Corresponding author. Tel.: +33 549 49 82 90; fax: +33 549 08 23 36.
E-mail address: trogaume@univ-poitiers.fr (T. Rogaume).

1290-0729/$ – see front matter © 2008 Elsevier Masson SAS. All rights reserved.
doi:10.1016/j.ijthermalsci.2008.02.003

Optimization of the combustion process is here the preferred approach. The physical basis for optimization is the minimization of NO emissions achieved through a reduction of the temperature of combustion and a reduction of the local concentration of oxygen. The temperature of combustion is directly dependent on the fuel/oxidizer ratio as well as the O_2 concentration. Therefore, the main variables used for the direct control of the NO emissions are the air flow rate and oxygen concentration. Commonly, the total air flow is divided in two: A fraction of the air flows through the fuel bed and is labeled the primary air the rest is introduced above the bed of solids and is called the secondary air. The primary combustion zone is then a temperature limited, fuel rich zone and the secondary combustion zone is characterized by a hotter and leaner reaction. Optimization of the combustion conditions requires then the optimization of the primary and of the secondary air flow rates. It is therefore of great importance to understand the individual effect of these two sources of oxygen.

The objective of this work is to study the influence of the primary and secondary air flows on the combustion process and the formation NO. Emphasis will be given to the effect of the primary and secondary flow on the characteristics of the combustion process, temperatures, mass loss rates and phenomenological observations. To reduce the number of variables the oxygen concentration has been kept as that of air and the experiments have been carried using a fixed-bed reactor. These simplifications eliminate the variable of fuel supply and limit possible changes in the pyrolysis of the fuel that could be attributed to surface oxidation. Thus, the present experiments correspond to a simplified scenario that, nevertheless, allows the independent study of both forms of air supply.

2. Experimental methodology

2.1. Definition of the fuel

In Europe, typical municipal solid waste consists primarily of wood, paper and cardboard, and plastics. In the present study an idealized and repeatable simulated-waste was used of composition 41% wood, 37% cardboard, 19% polyethylene terephtalate (PET) and 3% polyamide [10]. A chemical analysis has been done to verify if the idealized waste used simulates well the combustible part of municipal solid waste. Special care has been given to keep the nitrogen content as close to that of the waste (0.5%). This is essential since the nitrogen content has a significant impact on the yield of NO generated by means of the fuel mechanism [9–11]. The wood used is pine and is introduced in the form of pellets 10 mm by 5 mm. The cardboard is cut in pieces of 20 mm by 20 mm and the polyethylene in smaller pieces of 10 mm by 10 mm. The polyamide is introduced as granules. The wood and cardboard are dried for 24 hours at a temperature of 105 °C to eliminate all the moisture of the fuel, because for industrial incinerators, moisture is evaporated before the combustion, during the pre-heating. The sample weight is fixed for all tests to 1400 grams representing an initial depth of 80 cm in the furnace. It is important to notice that after the end of the combustion, the depth of char is about 3 to 4 cm.

2.2. Experimental set-up

The objective is to simulate the combustion of solid waste within a moving grate industrial incinerator. This process can be divided in three steps, an initial drying step, followed by gasification and ignition of the waste and finally by oxidation of the char and residues. The present experimental configuration attempts to emulate these stages within a fixed-bed counter-flow reactor which has been industrially validated by [13,14]. Once the fuel is in the reactor combustion is initiated at the top of the fuel, representing 80 cm depth. The waste then burns in a counter-flow propagation mode. The primary air flow comes from the bottom towards the top and the reaction front propagates downwards. This process does not follow a continuous operation mode but each batch of waste conforms to similar conditions as those found in a moving grate incinerator. On top of the fuel bed the secondary air is injected into the reacting zone to complete the combustion process. A detail of the reactor is presented [10] and a schematic in Fig. 1.

The ignition of the combustible is accomplished at the top of the solid by means of a small pilot flame (ignition pipe). Once ignition has been accomplished all flow rates are adjusted to the experimental values. The region immediately above the fuel, where combustion will occur, is labeled the secondary zone of combustion. At the moment of ignition this zone covers an approximate height of 1200 mm. The secondary air of combustion is injected in this zone using two tubes of 20 mm of inner diameter at three different heights, as shown by Fig. 1. As shown in Fig. 1 this zone will be further divided into a tertiary zone of combustion at the downstream end of the reactor. The primary and secondary air flow rates are fixed and measured using regulating mass flow meters. The primary air flow meter covers a range between 0 and 100 Nm^3/h and the secondary one between 0 and 50 Nm^3/h. The precision of the measure is 1% at the full scale.

Temperatures inside the combustion chamber are measured with 0.5 mm diameter type K thermocouples. Twenty-eight thermocouples are placed inside the reactor with their tip along the axis of the chamber. The distance between thermocouples is presented in Fig. 1. The combustion products are extracted from the exhaust pipe and analyzed by means of an electro-chemical analyzer make TESTOTERM model 350. This analyzer measures O_2, CO, NO, NO_2, SO_2. The precision of the measures given by the analyzer used is about $\pm 0.2\%$ concerning the O_2 and ± 20 ppm concerning the other gases analyzed. The CO_2 concentrations are calculated from a carbon balance under the assumption that there are no other carbon-containing products of combustion.

2.3. Experimental conditions

To establish the experimental conditions it was necessary to conduct preliminary experiments to establish the air flow rates

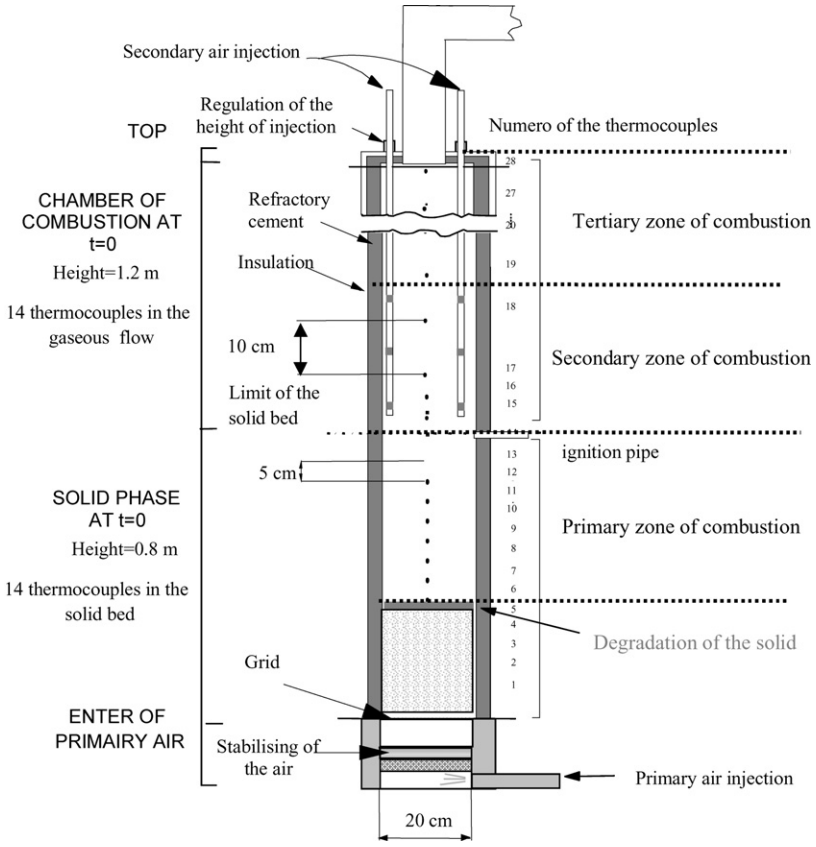

Fig. 1. Description of the fixed-bed reactor.

necessary for stoichiometric combustion. This is important because the air flow rate necessary for stoichiometric combustion will depend on the propagation velocity of the reaction front. Once an estimate of the air requirements for stoichiometric combustion has been made, then the primary air flow rate can be adjusted to provide a range of conditions that will extend from fuel rich to fuel lean. The preliminary set of experiments established that an average time of approximately 470 seconds was required for propagation of the reaction front all through the 1400 grams of fuel. By knowing the C/H/O/N/S composition of the mixture it is possible to estimate the average air flow rate necessary to obtain stoichiometric combustion [10,11], for this particular fuel is approximately 50 Nm^3/h. This flow rate will vary slightly for different experimental conditions since the propagation velocity is a direct function of the primary air flow rate, but was considered appropriate since the dependency of the propagation velocity on the air flow rate tends to be linear [14]. On the basis of this information the primary air was established within the range of 35 and 95 Nm^3/h and the secondary air was set to vary between 25 to 45 Nm^3/h. These values provided a range of 60 to 140 Nm^3/h for the total air supply. For practical reasons it is important to define a variable that will be representative of the global incineration process and will include both air supplies and the propagation rate. This is of significant importance in the normalization of the pollutant species, because all measurements are made at the end of the process. For this purpose a variable named the "excess air" is defined as the ratio of the air flow rate injected to that necessary for stoichiometric combustion. The former value is known being the test parameter and the latter is obtained, as explained earlier, from the measured propagation velocity and the chemical composition of the mixture [15]. This value is determined by several assumptions and observation:

- it is calculated from the mass loss rate of the solid fuel during the established combustion so from the time necessary to burn the (initial mass (1400 g)—mass of char at the end) grams of combustible. The mass as well as the delay of combustion is determined for each experiment;
- past results have shown that the consumption of oxygen due to the char (uncombusted carbon) oxidation is negligible.

The "excess air" is a form of equivalence ratio because it takes into account the propagation rate, and thus the fuel contribution [10]. This parameter will be used during the discussion of the results. A minimum of three repeat tests have been performed for each experimental condition in order to verify the repeatability of the experiments showing a maximum deviation of 10% from the average values. The results presented in the following sections correspond to the average values. For simplicity no error bars will be presented and therefore the range of data can be assumed as being always less than 10% from the presented.

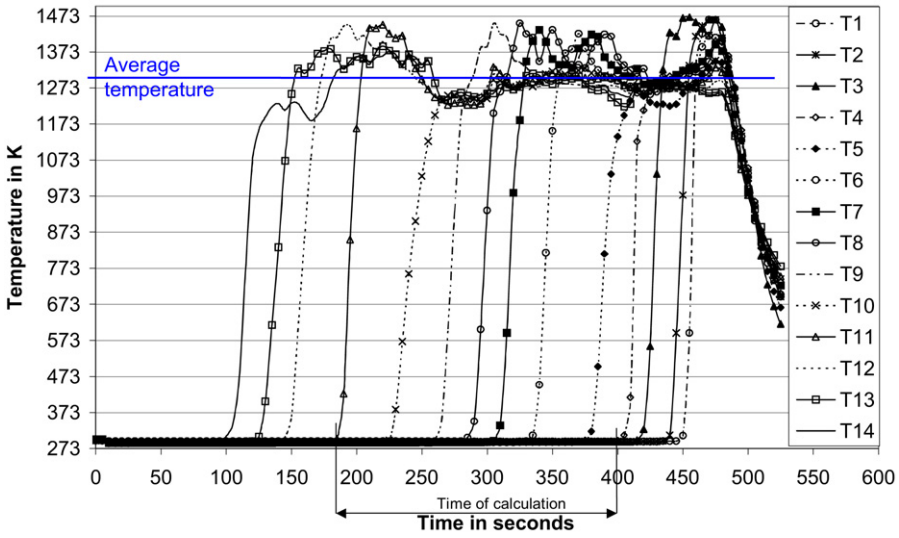

Fig. 2. Example of a set of temperature histories in first zone of combustion ($Q_1 = 60$ Nm^3/h and $Q_2 = 35$ Nm^3/h). Q_1: primary air flow; Q_2: secondary air flow.

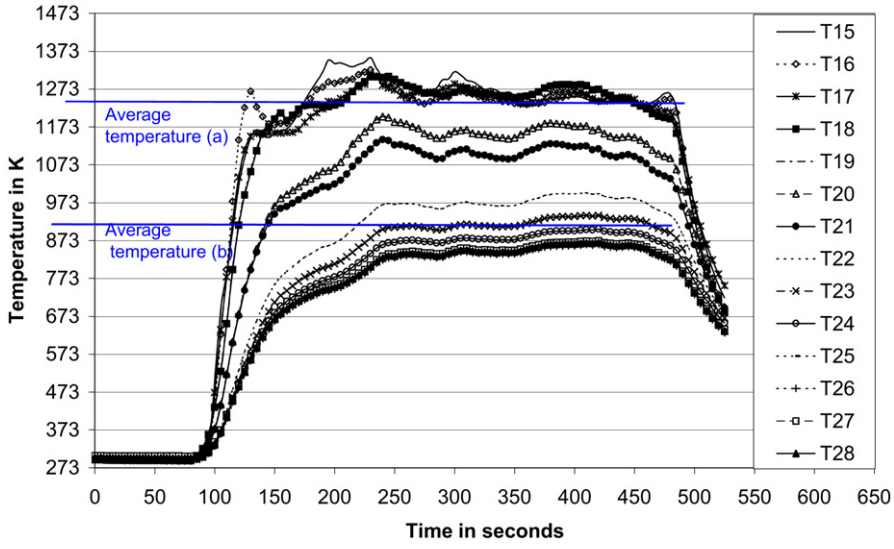

Fig. 3. Example of a set of temperature histories in second zone of combustion (primary air $Q_1 = 60$ Nm^3/h and secondary air $Q_2 = 30$ Nm^3/h).

3. Experimental results

3.1. Description of the combustion process

Once ignition is achieved the reaction front propagates downwards through the fuel bed. Therefore, the secondary zone of combustion increases in size. A representative set of temperature histories is presented in Fig. 2. Fig. 2 shows that before ignition all thermocouples are at ambient temperature, once ignition occurs the temperature increases suddenly until it reaches a peak value, once this value has been reached the thermocouple traces oscillate in a random fashion. These oscillations are representative of the thermocouple having emerged from the solid fuel. From Fig. 2 it can be seen that the temperature reaches a peak then it descends to a lower plateau within a period that varies between 100–200 seconds. Once this plateau is reached temperatures oscillate within a smaller band. For this study, the average temperature is defined as the time average of all temperature values recorded after the peak value. An example is presented in Fig. 2. The fourteen thermocouple traces recorded from the solid are presented in Fig. 2. All thermocouples follow a similar pattern and are separated by an almost constant time lag. This denotes a constant propagation velocity. After the reaction front has reached the final thermocouple the temperatures drop suddenly denoting the end of the combustion process.

Fig. 3 shows a representative plot of the temperature histories within the gas phase. The temperature distributions correspond to the same case as Fig. 2.

As can be seen from the curve the temperatures increase suddenly after ignition. Attainment of steady state temperatures takes approximately 200 seconds after ignition. Beyond that period, little temperature variation can be observed. Finally, the temperatures decay as the reaction front reaches the end of the sample (Fig. 2). Thermocouples 15–21 correspond to the region where the secondary air is injected and thermo-

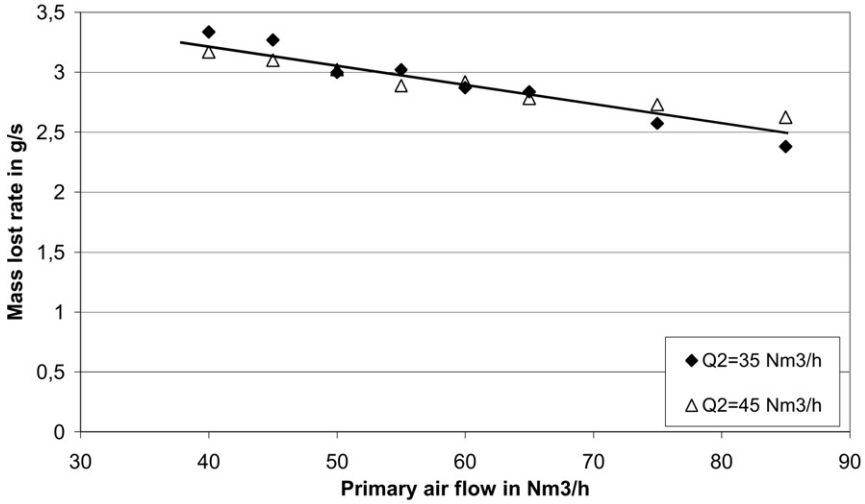

Fig. 4. Evolution of the mass loss rate as a function of the primary air flow rate.

couples 22 to 28 to the region immediately downstream. The temperatures measured within the region of air injection are almost constant showing an uniform reaction zone albeit the fact that thermocouple 15 is separated 0.5 m from thermocouple 21. Downstream of thermocouple 21, combustion seems to decrease in intensity and slow temperature decay becomes evident as the gases migrate through the reactor. The final thermocouples show that the combustion products have almost attained thermal equilibrium showing the well-insulated nature of the reactor. The temperature histories depicted in Fig. 3 show that it is important to divide the region above the fuel into two distinct zones. The secondary zone of combustion is the reactive region and the tertiary zone of combustion corresponds to the end of the exothermic reaction of oxidation (temperature decay). For purposes of comparison average temperatures will be established independently for both zones and will be calculated by means of the time average of all temperature data recorded after the initial transient period and before extinction. The temperature into the secondary zone of combustion is determined the average temperature (a) Fig. 3, then average temperature (b) correspond to the temperature into the third zone of combustion. Examples of these average temperatures are presented in Fig. 3.

3.2. Evolution of the mass loss rate

The evolution of the propagation velocity of the reactive front was studied as a function of the primary and secondary air flow rates. The data will not be presented as a propagation velocity but as a mass loss rate. By multiplying the propagation velocity by the average density of the waste and the surface area of the reactor a mass loss rate can be obtained. This choice of presentation is made because the efficiency of an incineration furnace is given by the rate at which mass of waste can be converted. The rate of pollutant formation, therefore, has to be normalized by the rate at which the mass of waste is lost. Optimization of pollutant formation has to be done on the basis of mass of pollutant per unit mass of waste converted.

Fig. 4 shows a series of mass loss rates for different primary air flow rates. Data are presented for two different secondary air flow rates. As predicted by theory Zhou et al. [14], the mass loss rate is inversely proportional to the mass of air flowing through the reactor. The heat feedback from the flames to the fuel is primarily controlled by radiation, therefore provides a constant heat flux boundary condition for the mass of fuel and oxidizer moving towards the reaction front. The propagation rate is therefore insensitive to the nature of the combustion region. Further evidence of this is provided by the insensitivity of the mass loss rate to the secondary air flow rate. Fig. 4 presents only two specific conditions but mass loss rate data for all other secondary air flow rates fall within the same line. These observations are very important for modeling since they attest to a parabolic problem, where the reaction can be treated as an evolving control volume that is not affected by the downstream conditions.

As explained earlier, the mass loss rate presented in Fig. 4 can be used to calculate the stoichiometric requirement of air for each experimental condition. Therefore, all data presented in the following sections will be normalized and presented as total excess air (e_T). The total excess air can be subdivided into excess primary air (e_1) and excess secondary air (e_2). During this study, the primary excess air was varied from $e_1 = 0.6$ to 2.5 and the secondary excess air between $e_2 = 0.5$ to 1.2, thus the total excess air ranged between $e_T = 1.1$ to 3.7.

3.3. Gaseous emissions

Throughout this section the recorded emissions of NO will be presented as a function of the excess air. The data symbols will discriminate between the different primary excess air quantities used. The emissions of NO obtained are presented in mg of product formed per gram of combustible burned. The mass of solid consumed is obtained from Fig. 4. Measurements of NO emissions are presented in Fig. 5 and in Fig. 6 for the CO emissions.

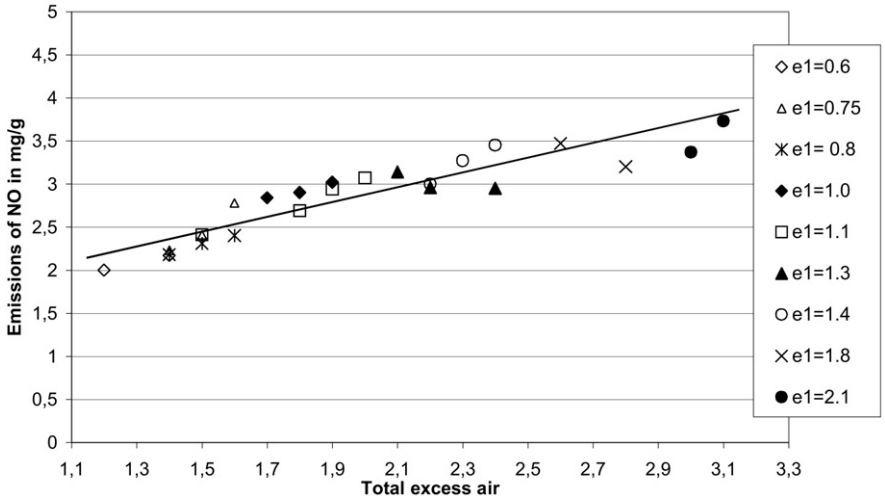

Fig. 5. Variation of the emissions of NO as a function of the total excess air.

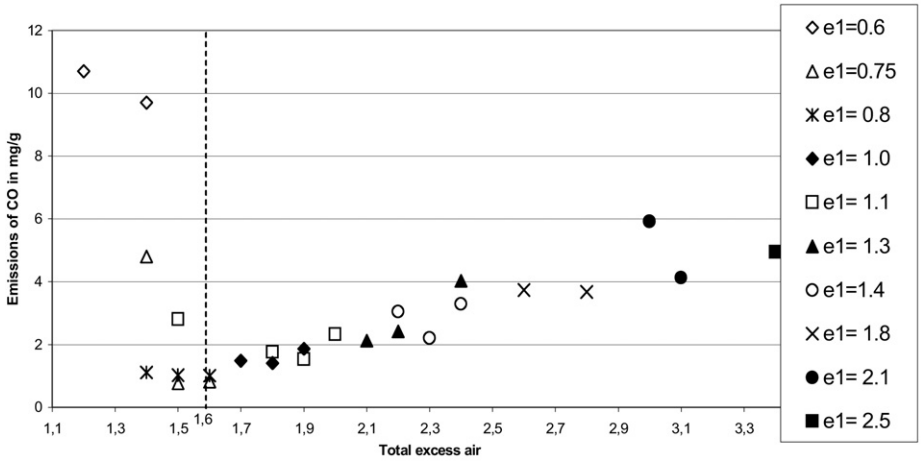

Fig. 6. Variation of the emissions of CO as a function of the total excess air.

Fig. 5 shows a clear linear dependency of NO production with the total excess air. Independent of where the contribution is made (primary or secondary air), the yield of NO depends on the total air available. In contrast, Fig. 6 shows two well defined regimes, for $e_T < 1.6$ the yield of CO decreases rapidly with the total excess air. It is important to note that a total excess air $e_T = 1.6$ corresponds to a primary excess air $e_1 = 1$. For $e_T > 1.6$ the production of CO follows a weak linear relationship with the excess air. Thus, the minimum yield of CO occurs approximately at $e_T = 1.6$. Furthermore, the data for $e_T < 1.6$ (so $e_1 < 1$) shows a very strong dependency on the primary air. A small increase in the primary air results in a strong decrease in the yield of CO. For $e_T > 1.6$ (so $e_1 > 1$) the dependency of the yield on CO seems to be only on the total excess air and not on the individual sources of oxygen.

3.4. Combustion regimes

The concentrations of CO have shown the presence of two distinct combustion regimes. The change in regime does not seem to affect the production of NO that seems to follow a linear relationship with the total excess air. Nevertheless, it is essential to try to understand the characteristics of the different combustion modes and assess their impact on the formation of CO and NO.

The primary indicator of the characteristics of the combustion process is the temperature. Fig. 7 shows the evolution of the temperature with the excess air for the primary zone of combustion. Fig. 9 presents the same information for the secondary zone of combustion. The data are presented as a function of the excess air but the symbols discriminate between the different primary excess-air.

Fig. 7 shows the same two regimes evidenced by the CO measurements and depending of the value of the primary excess air, inferior or superior to 1. For $e_1 < 1$ (represented here by $e_T < 1.6$) the characteristic temperature of the primary zone of combustion is scattered around 1100 K, for $e_1 > 1$ ($e_T > 1.6$), the scattering of the data is reduced and the average temperature rises to approximately 1250 K. For $e_1 < 1$, an increase in primary air seems to lead to a slight increase in the temperature while for a constant primary air an increase in the secondary air results in a decrease in temperature. Nevertheless the scatter of the data does not allow establishing these trends with certainty.

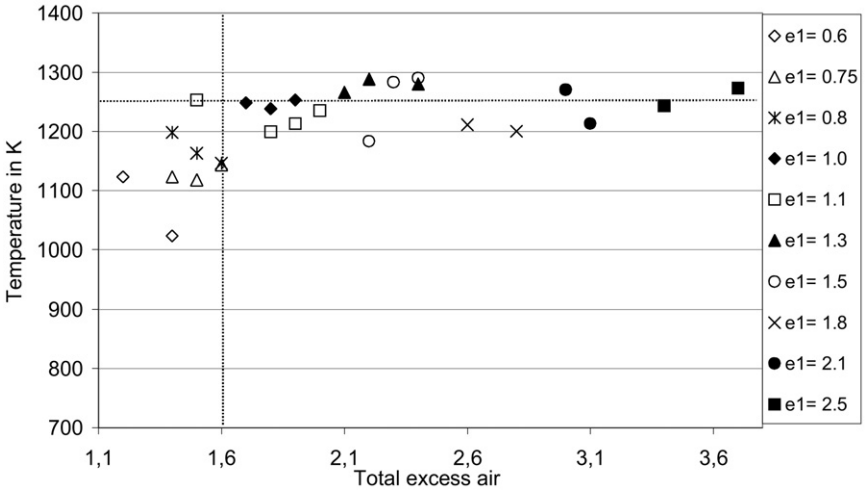

Fig. 7. Influence of the total excess air on the average temperature in the primary zone of combustion.

For $e_1 > 1$ no evident trends with the primary or secondary air seem to prevail.

To better explain these two combustion regimes individual temperature histories for the primary zone of combustion have been selected for a case where $e_1 < 1$ (and $e_T < 1.6$) and one where $e_1 > 1$ (and $e_T > 1.6$). These temperature histories are presented in Fig. 8 and will be considered representative of all other experimental conditions. The specific location of each thermocouple used on Fig. 8 are given in Fig. 1.

Fig. 8(a) is characteristic of a combustion with a primary excess air $e_1 < 1$ and a total excess air $e_T < 1.6$. It is divided in 5 time intervals labeled 1 to 5. The initial interval precedes the arrival of the thermal wave and is characterized by a constant ambient temperature. Approximately 120 seconds from ignition the thermal wave reaches the thermocouple and a sudden increase in temperature follows. At approximately 130 seconds from ignition a visible decrease in slope can be established from the temperature history. This slower temperature rise is characteristic of strong endothermic degradation of the fuel. The temperature at which this change in slope occurs (~673 K) is also characteristic of the pyrolysis of materials similar to the ones used in this study. This slope change is presented in Fig. 8(a) as the transition between zones 2 and 3 and labeled pyrolysis step. This particular temperature history corresponds to $e_1 < 1$, therefore the gasification of the fuel is expected to occur under a low oxygen concentration. A decrease in oxygen concentration tends to favor endothermic pyrolysis pathways and thus result in a decrease in the slope of the temperature histories. Visual observation of the combustion chamber showed that for this particular regime the reaction migrated to the interior of the porous matrix where endothermic pyrolyis competes with exothermic oxidation.

The original slope is recovered approximately 20 seconds later and the temperature continues to increase until it reaches the combustion temperature (~1125 K). At this point the temperature remains constant throughout the combustion process. It is important to note that at this point the thermocouple is outside the porous media and in the gas phase. The temperature increases when the reaction front has reached the end of the reactor (480 second). At this point there is a final increase of temperature that can be attributed to a change in stoichiometry generated by the small amount of fuel left, a secondary reaction originated by oxidation of the char or an end effect. This increase marks the end of combustion and is followed by cool down. It is important to note that since $e_1 < 1$ the final increase in temperature is most likely associated to a variation of the fuel/oxidizer ratio towards stoichiometric conditions.

These observations are of great importance since they show that reducing the primary air below the stoichiometric requirement leads to a combustion regime that will favor the formation of carbon monoxide.

For a temperature history corresponding to $e_1 > 1$ and $e_T > 1.6$ (Fig. 8(b)) it can be observed that similar zones can be established. The notable differences are the absence of the pyrolysis step and of the final temperature peak. In this particular case, gasification occurs in an oxygen rich environment and combustion occurs in the gas phase. This results in an earlier temperature peak that occurs at approximately 200 seconds. This peak corresponds to a narrow reactive zone occurring above the fuel. A plateau at a temperature that is representative of the combustion products follows. This combustion regime, where the reaction front emerges to the gas phase, results in a significant reduction in the yield of CO.

For the secondary zone of combustion the temperature increases with the excess air $e_T < 1.6$, reaches a plateau, $1.6 < e_T < 2.4$, and then decays, $e_T > 2.4$ (Fig. 9). For $e_1 < 1$ ($e_T < 1.6$) there is no evident trend with the individual sources of air but the temperature seems to increase with the secondary excess air. As the temperature reaches the plateau, the second zone of combustion seems to remain unchanged with the primary air and to increase with the secondary air. This observation is consistent with the mass loss curves. The fuel mass loss is proportional to the primary air so a change in this component of the airflow velocity will have no effect on the stoichiometry of the secondary zone of combustion. For $e_1 > 1$, the overall reaction is fuel lean therefore an increase in the total air flow should result in a decrease in temperature. Nevertheless, for $1.6 < e_T < 2.4$ an increase in the secondary flow leads to an

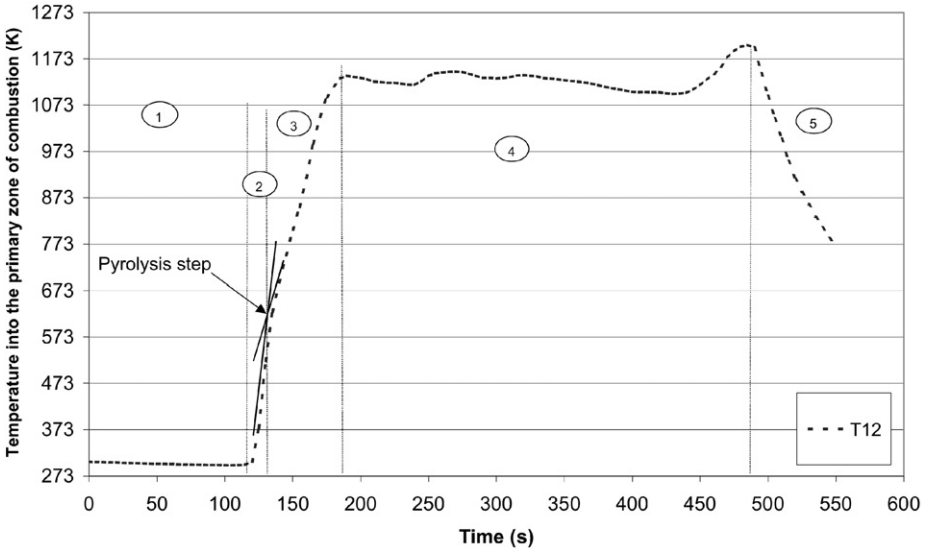

(a)

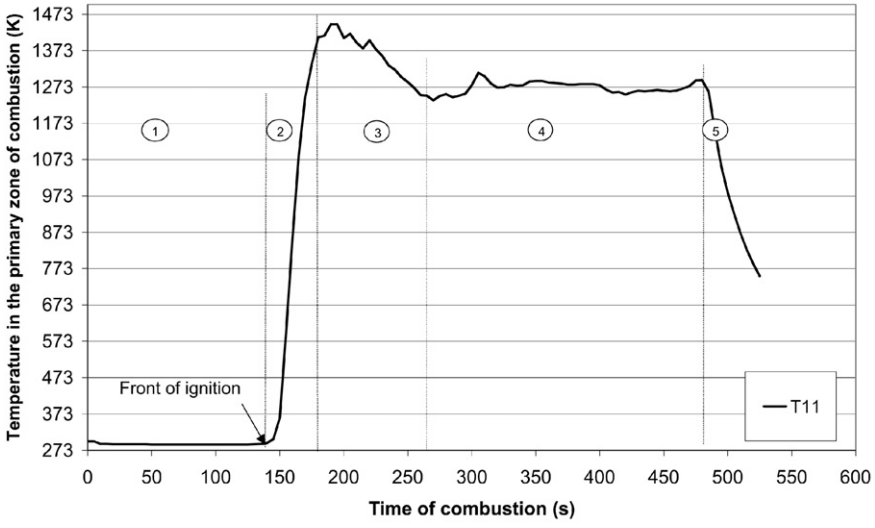

(b)

Fig. 8. Individual temperature history within the primary zone of combustion. (a) Primary airflow of 45 Nm^3/h and a secondary airflow of 45 Nm^3/h, therefore $e_1 = 0.75$, $e_T = 1.5$. (b) Primary air flow of 60 Nm^3/h and secondary air flow of 45 Nm^3/h, therefore $e_1 = 1.3$, $e_T = 2.3$.

increase in temperature. A plausible explanation to this behavior is that an increase in airflow results in an increased mixing within the secondary zone of combustion. For $e_T > 2.4$ the enhancement of mixing becomes less important and the stoichiometry controls the reaction temperature. Under these conditions an increase in the secondary airflow leads to a decrease in temperature.

The temperatures of the primary and secondary zones of combustion have shown that the presence of independent regimes for both zones. The primary zone is controlled by the primary airflow which generates two distinct combustion regimes, where $e_1 = 1$ and $e_T = 1.6$ seems to be respectively the critical primary and total excess air. Furthermore, these different regimes lead to significantly different trends on the yield of CO. The characteristics of secondary zone of combustion are also affected by this change of regime. For $e_1 < 1$ ($e_T < 1.6$) the fuel content reaching the secondary zone seems to be given by the combustion regime in the primary zone, nevertheless the burning conditions are mostly controlled by mixing. Mixing seems to dominate until the total excess air reaches approximately 2.4. At this point the stoichiometry seems to become the dominant parameter.

4. Conclusion

An experimental study has been conducted with a fixed-bed reactor to simulate, in a laboratory scale, industrial municipal waste incineration using moving grates. The present study has concentrated on the observation of the different combustion regimes and their impact on the production of NO. It can be concluded that:

- The amount of primary air introduced through the fuel has a significant effect in the nature of the combustion process. Two different regimes have been identified. For air flow

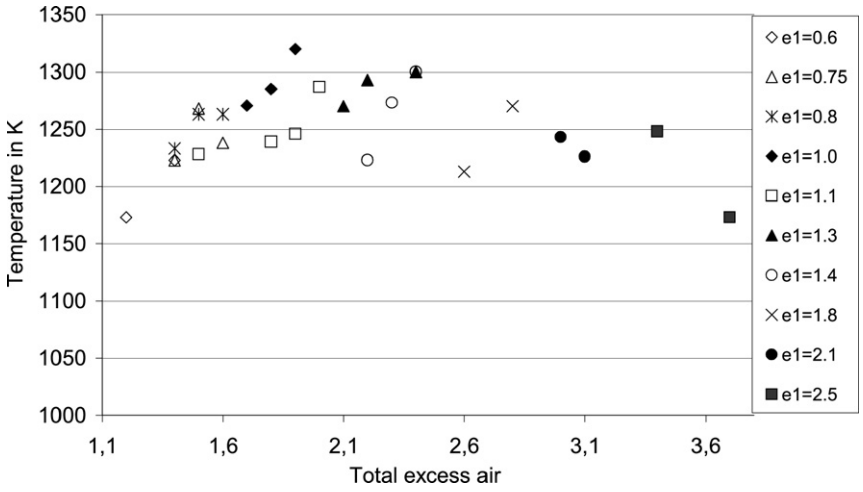

Fig. 9. Influence of the total excess air on the average temperature in the secondary zone of combustion.

rates below the stoichiometric requirement an oxygen deficient combustion regime is established within the porous matrix. This regime is characterized by low reaction temperatures, and favors endothermic pyrolysis.

- For a total excess air below 2.4 mixing controls the reaction between the secondary air and the products of the primary zone of combustion. An enhancement of the secondary air results in better mixing and an increase in temperature.
- For a total excess air greater than 2.4 the enhancement of mixing becomes less important and the stoichiometry controls the reaction temperature. Under these conditions an increase in the secondary air flow rate leads to a leaner mixture and a decrease in temperature.
- Under the present experimental conditions the production of NO seems to be controlled only by the oxygen concentration in the secondary zone of combustion. An increase in total excess air flow rate results in an increase in the yield of NO.

Acknowledgements

The financial supports of this work by the Agence De l'Environnement et de la Maitrise de l'Energie (ADEME) and by the Centre de Recherche pour l'Environnement l'Energie et le Déchet (CREED) are gratefully acknowledged.

References

[1] C. Koshland, Impacts and control of air toxics from combustion, in: 26th International Symposium on Combustion, The Combustion Institute, 1996, pp. 2049–2065.
[2] J.S. Lighty, J.M. Vernath, The role of research in practical incineration systems – a look at the past and the future, in: 27th International Symposium on Combustion, The Combustion Institute, 1998, pp. 1255–1273.
[3] T. Abbas, P. Costen, F.C. Lockwood, A review of current NOx control methodologies for municipal solid waste combustion process, in: 4th European Conference on Industrial Furnaces and Boilers, London, 1997.
[4] Y.B. Zeldovitch, The oxydation of Nitrogen in combustion and explosions, Acta Physicochemica, USSR 21 (1946) 577–628.
[5] C.P. Fenimore, Formation of nitric oxide in premixed hydrocarbon flame, in: 13th International Symposium on Combustion, The Combustion Institute, 1970, pp. 373–380.
[6] G.G. De Soete, Overall reaction rates of NO and N_2 formation from fuel nitrogen, in: 15th Symposium International on Combustion, The Combustion Institute, 1974, pp. 1093–1102.
[7] J.A. Miller, C.T. Bowman, Mechanism and modeling of nitrogen chemistry in combustion, Progress Energy Combustion Science 15 (1989) 287–338.
[8] S. Kim, D. Shin, S. Choï, Comparative evaluation of municipal solid waste incinerator designs by flow recirculation, Combustion and Flame 106 (1996) 241–251.
[9] G.G. De Soete, Mécanismes de formation et de destruction des oxydes d'azote dans la combustion, Revue Générale de Thermique 330–331 (1989) 353–373.
[10] T. Rogaume, M. Auzanneau, F. Jabouille, J.C. Goudeau, J.L. Torero, The effects of different airflows on the formation of the pollutants during waste incineration, Fuel 81 (2002) 2277–2288.
[11] T. Rogaume, M. Auzanneau, F. Jabouille, J.C. Goudeau, J.L. Torero, Computational model to investigate the effect of different airflows on the formation of pollutants during waste incineration, Combustion Science and Technology 175 (2003) 1501–1533.
[12] L. Sorum, O. Skreiberg, P. Glarborg, A. Jensen, K.D. Dam Johansen, Formation of NO from combustion of volatiles from municipal solid wastes, Combustion and Flame 123 (2001) 195–212.
[13] X. Zhou, Contribution à l'étude de l'incinération des déchets urbains: expérimentation en réacteur à lit fixe à contre courant, approche théorique du déplacement du front d'inflammation, Thèse de Doctorat de l'Université de Poitiers, 1994.
[14] X. Zhou, J.L. Torero, J.C. Goudeau, B. Bregeon, On the propagation of a reaction front through a porous fuel in the presence of an opposed forced flow: application to mixtures characteristic of municipal waste, Combustion Science and Technology 110–111 (1995) 123–146.
[15] T. Rogaume, Caractérisation expérimentale et modélisation de l'émission des polluants lors de l'incinération des déchets ménagers, Thèse de doctorat de l'université de Poitiers, 2001.